Thin-Walled Structures 62 (2013) 206–214

Contents lists available at SciVerse ScienceDirect

Thin-Walled Structures

journal homepage: www.elsevier.com/locate/tws

Computational evaluation of limit states of thin-walled channels made from steel foam

Mohammadreza Moradi [a], Sanjay R. Arwade [b,*], Benjamin W. Schafer [c]

[a] 113D CNAS, University of Guam, Mangilao 96923, Guam
[b] 223 Marston Hall, Amherst, University of Massachusetts, MA 01003, United States
[c] 208 Latrobe Hall, Johns Hopkins University, Baltimore, MD 21218, United States

ARTICLE INFO

Article history:
Received 27 June 2012
Accepted 5 July 2012

Keywords:
Steel foam
Elastic buckling
Nominal strength
Steel foam
Local buckling
Distortional buckling
Thin-walled channel

ABSTRACT

The objective of this paper is to explore the potential strength and serviceability implications of metallic foams, specifically steel foam, utilized as a thin-walled channel structural member. A typical advantage sought in the selection of a thin-walled member is minimal weight. However, the stability of the thin walls and the related limit states constrains the extent to which weight minimization may be utilized. As a material, steel foam (literally creating air voids in the steel microstructure) offers the potential to provide increased plate stiffness for a given weight and thus create even lighter thin-walled members and structures. In this work analytical material relationships are used to explore the structural potential for steel foam. First, the local buckling and yielding of an isolated steel foam plate is explored. Second, the local, distortional, and global buckling of a prototypical cold-formed steel channel using steel foam is examined. Finally, the strength and governing limit state of the channel as a function of relative density (i.e., the degree to which the material is foamed) is explored. The results show the key tradeoff made when foaming–stiffness per weight is increased, including stiffness related to member buckling modes; however, yield strength per weight decreases. Depending on the slenderness (in local, distortional, and global modes) of the member this tradeoff can be beneficial or detrimental.

1. Introduction

Thin-walled cold-formed steel lipped channels are commonly used in a variety of structural applications such as load-bearing and non-load bearing wall studs, floor joists, purlins, and girts. A key advantage of these structural members is that they are lightweight and easy to work with during field assembly. To achieve such lightness the walls of the folded member are thin, typically less than 2 mm, and as a result of this thinness plate instability is a common limit state.

In this study, we explore the possibility of lipped channels in which the member is formed from steel foam, rather than thin solid steel sheet. Steel foam has been developed over approximately the past 20 years and is now a mature material at laboratory production scales [1–3]. The material shares many similarities in microstructure and material properties with foams using metals such as aluminum and titanium as a base metal. These similarities include the possibility of open or closed cell microstructures, high elastic modulus to weight ratios, and stress–strain curves exhibiting a well defined yield point and long compressive plateau [15]. Because the microstructure of steel foam is similar to that of other metal foams, analytical equations linking the relative density and elastic modulus/yield stress [5] can be applied to steel foams. This is supported by the findings of a recent review paper on steel foam microstructure and mechanical properties [15]. By virtue of using steel as the base metal, steel foams promise greater eventual economy of scales and easier integration into civil structures due to the manufacturing and design infrastructure already in place for the use of steel. The steel foam lipped channels described here represent the first such candidate application.

This study examines, by analytical and empirical equations and numerical simulation, the behavior of two types of structural members made of steel foam: flat plates and thin-walled lipped channels. In both cases steel foams with relative density ranging from 1.0 (solid steel) to 0.05 (a very light steel foam) are examined, and the thickness of the steel foam plates or sections is chosen such that the unit weight is the same as for an equivalent solid steel plate or section.

To investigate the behavior of steel foam plates, exact expressions for the plate bending rigidity, elastic buckling capacity, and

* Corresponding author.
E-mail addresses: mremoradi@gmail.com (M. Moradi), arwade@ecs.umass.edu (S.R. Arwade), schafer@jhu.edu (B.W. Schafer).

0263-8231/$ - see front matter © 2012 Elsevier Ltd. All rights reserved.
http://dx.doi.org/10.1016/j.tws.2012.07.007

crush loads are used. Winter's equation [16], a semi-empirical expression, is used to combine the elastic buckling capacity and crush loads into the plate strength. Although Winter's equation is semi-empirical, not exact, it is widely used in design to evaluate the capacity of plates loaded in-plane, and it is used here to show that steel foam plates provide advantages in a structural engineering design context.

For thin-walled lipped channels, the finite strip method is used to evaluate the elastic buckling capacity of steel foam lipped channels and the Direct Strength Method is used to evaluate member strength. The finite strip method is a well established numerical technique for the instability analysis of thin-walled sections. The method is accepted for design by the specification of the American Iron and Steel Institute (AISI), and gives results equal to those obtained by the finite element method while consuming far fewer computational resources. The semi-empirical Direct Strength Method is encoded in the AISI specification, and is essentially a method of strength calculation for thin-walled members that is parallel in theoretical support and structure to Winter's equation [17].

2. Material and geometrical properties of the steel foam sections

To hold the weight per unit length of the cross section constant, while reducing the relative density of the walls (i.e. replacing the solid steel walls with steel foam walls), the thickness of the cross section has to be increased. The weight per unit length and per unit width of the solid steel and steel foam walls are $t_f\rho_f$ and $t_s\rho_s$ respectively, where t_f and t_s are the steel foam and solid steel wall thickness, and ρ_f and ρ_s are the steel foam and solid steel weight densities. The constraint on the weight per unit length of the member can then be expressed as $t_f\rho_f = t_s\rho_s$. By replacing the ratio ρ_f/ρ_s by ρ, the relative density of the foam, we find that

$$t_f = \frac{t_s}{\rho} \tag{1}$$

which relates the thickness of the steel foam walls to the thickness of the solid steel walls.

The material properties of metallic foams are different from those of solid metals and depend on base metal properties and relative density. Ashby and Gibson [10] developed the expressions

$$E_f = E_s\rho^2 \tag{2}$$

and

$$f_{yf} = f_{ys}\rho^{1.5} \tag{3}$$

Extending the preceding to steel foam: the elastic modulus and yield stress of steel foam is related to the elastic modulus and yield stress of solid steel and relative density [5]. In these equations subscripts s and f stand for solid steel and steel foam properties respectively. While a reduction in relative density results in lower elastic modulus and yield stress, the rates at which these two properties decrease differ. This difference plays a crucial role in determining how the relative density of the steel foam influences the buckling response of the thin plates and lipped channels.

3. Steel foam plate

Before investigating the behavior of the steel foam lipped channel, it is worthwhile to study the behavior of a simple steel foam plate since the walls of the lipped channel behave in many ways as thin plates. The web plate of the 362S162-68 lipped channel [6] has width and thickness equal to 92.08 mm (3.625 in) and 1.73 mm (0.068 in) respectively, and is chosen for this part of the study. Simply supported boundary conditions are assumed along the four plate edges. The steel elastic modulus and steel yield stress are chosen to be equal to $E_s = 2.03 \times 10^5$ MPa (29 500 ksi) and $f_{ys} = 345$ MPa (50 ksi) respectively. The post-yielding behavior is assumed to be perfectly plastic.

3.1. Compression–moment failure interaction of steel foam plate

The plastic moment of a plate (M) (assuming simple one-dimensional behavior to develop basic relations for comparison) is a function of axial force (P), material property of the plate and geometry of the plate, and is given by

$$M = \left(\frac{t_f^2}{4} - \frac{P^2}{4b^2 f_{yf}^2}\right) b f_{yf} \tag{4}$$

in which t_f is the plate thickness and f_{yf} is the material yield stress. By substituting plate thickness and plate yield stress (Eqs. (1) and (3)) into Eq. (4), the plate plastic moment can be written in terms of steel foam relative density. This expression is

$$M = \frac{b f_{ys} t_s^2}{4\sqrt{\rho}} - \frac{P^2}{4 b f_{ys} \rho^{1.5}} \tag{5}$$

Two extreme cases of this interaction surface are the plastic moment (M_p) with no axial force, which is

$$M_p = \frac{b f_{ys} t_s^2}{4\sqrt{\rho}} \tag{6}$$

and the crushing load (P_{nf}) for zero moment, which is

$$P_{nf} = f_{ys} t_s b \sqrt{\rho} \tag{7}$$

Fig. 1 shows the compression–moment failure interaction surface for the steel foam plate. In part (a) of the figure, a section through

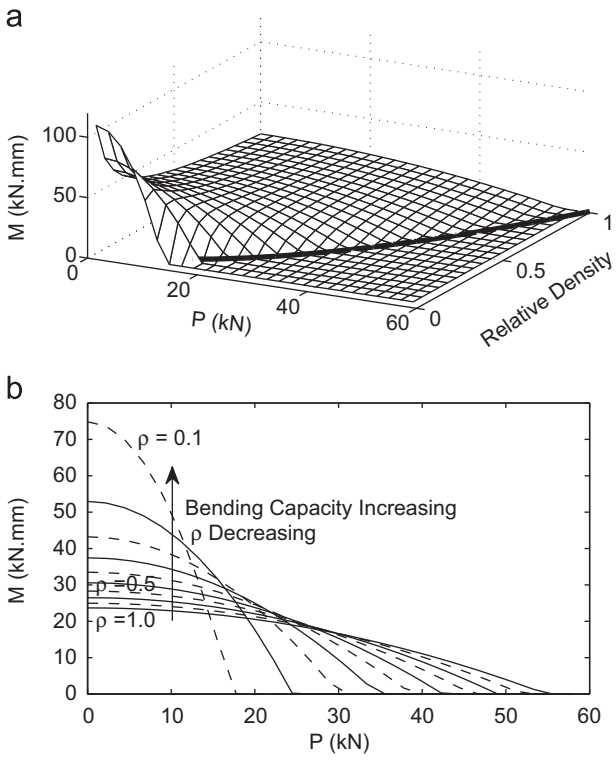

Fig. 1. Axial force–bending moment failure interaction surface of the steel foam plate (a) in 3D and (b) in 2D.

the plotted surface at constant relative density (ρ) gives a standard interaction diagram for the yield strength of a plate loaded in combined bending and in-plane compression. Part (b) shows several of those sections (interaction diagrams) so that the effect of relative density on bending and in-plane capacity can be more easily seen. The heavy line in part (a) represents the boundary at which in-plane crushing of the plate dominates. As the figure (especially part (b)) shows, a decrease in relative density is directly related to an increase in bending capacity and a decrease in in-plane capacity. For mixed mode loading the response depends on the proportion of in-plane and moment loading that is applied.

3.2. Steel foam plate rigidity and yield strength

In the expressions for the plate rigidity of solid steel and steel foam plates,

$$D_s = \frac{E_s t_s^3}{12(1-\nu^2)}$$
$$D_f = \frac{E_s t_s^3}{12(1-\nu^2)\rho} \tag{8}$$

the relative density ρ appears in the denominator, so that D_f, which is proportional to the buckling resistance of the steel foam plate, increases with decreasing relative density. This implies that a steel foam plate will have greater bending rigidity and elastic local buckling capacity than a solid steel plate of the same weight.

As it can be seen in Eq. (7), the crushing load of a steel foam plate is proportional to steel foam relative density. Therefore, a steel foam plate would be expected to have a smaller crushing (yielding) resistance to in-plane loading than a solid steel plate of the same weight.

3.3. Nominal strength of the steel foam plate

There are three collapse modes for a plate under pure compression: crushing, inelastic buckling, and elastic buckling. The nominal strength for a plate under pure compression may be expressed by Winter's equation

$$f_{winter} = \begin{cases} 1, & \lambda_f \le 0.673 \\ \dfrac{1-0.22/\lambda_f}{\lambda_f}, & \lambda_f > 0.673 \end{cases} \tag{9}$$

Eqs. (10) and (11) show the expressions for plate slenderness and simply supported buckling stress respectively which are substituted into Winter's equation:

$$\lambda_f = \frac{f_{yf}}{f_{crf}} \tag{10}$$

$$f_{crf} = \frac{4\pi^2 E_f t_f^2}{12(1-\nu^2)b^2} \tag{11}$$

If $\lambda_f \le 0.673$ the collapse mechanism is crushing and if $\lambda_f > 0.673$ the collapse mechanism is buckling. In the buckling zone if the nominal strength defined by Winter's equation is smaller than the buckling stress (Eq. (11)) the collapse mechanism is considered to be inelastic buckling and if the nominal strength is larger than buckling stress the collapse mechanism is elastic buckling (with postbuckling reserve).

By substituting the thickness and elastic modulus of the steel foam plate (Eqs. (1) and (2)) into Eq. (9), the nominal strength of the steel foam plate ($f_{winter} t_f b$) can be written in terms of the steel foam relative density. The ratio of nominal strength of the foam section (f_{winter}) to yield strength of the solid plate ($f_{ys} t_s b$) is defined as a normalized collapse load (*NCL*). Fig. 2 shows the

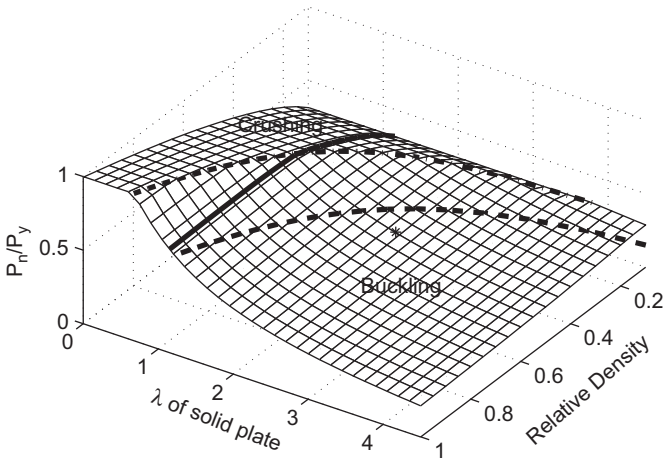

Fig. 2. Normalized plate collapse load in terms of solid plate slenderness and relative density (**–** plate with slenderness equal to 1.15, **-.-** intersection of crushing surface and inelastic buckling surface, **- -** intersection of inelastic buckling surface and elastic buckling surface).

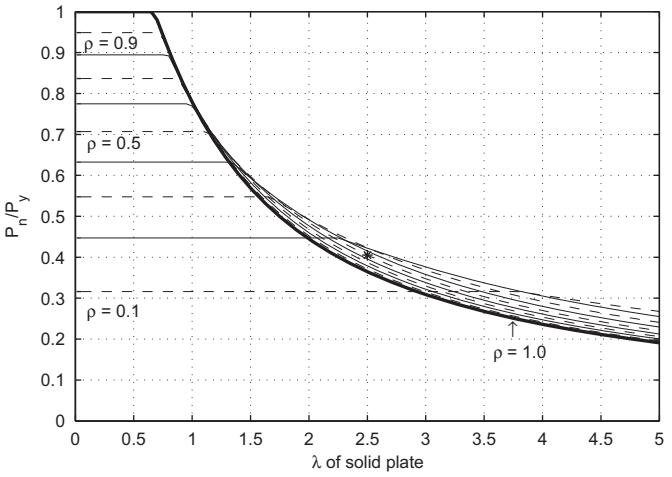

Fig. 3. Normalized plate collapse load in terms of solid plate slenderness and relative density. The curves get lower as the relative density is dropping.

normalized plate collapse load in terms of plate slenderness and relative density as a nominal strength surface and Figs. 3 and 4 show the corresponding curves obtained by fixing either the relative density or slenderness. The equation of the surface in Fig. 2 is

$$NCL = \begin{cases} \sqrt{\rho}, & \lambda \le \dfrac{0.673}{\rho^{0.75}} \\ 1-\dfrac{0.22}{\lambda\rho^{0.75}}, & \lambda > \dfrac{0.673}{\rho^{0.75}} \\ \dfrac{\lambda\rho^{0.25}}{\lambda\rho^{0.25}}, & \end{cases} \tag{12}$$

The solid line which is superimposed on the nominal strength surface corresponds to an example plate with slenderness equal to 1.15 and the dash-dot line **-.-** separates crushing and inelastic buckling. The equation for the solid line is

$$\lambda = \frac{0.673}{\rho^{0.75}}, \quad RP_{cb_e} = \sqrt{\rho} \tag{13}$$

and for the dash-dot line is

$$\lambda = \frac{0.78}{\rho^{0.75}}, \quad RP_{b_e b_i} = \frac{1}{\rho\lambda^2} \tag{14}$$

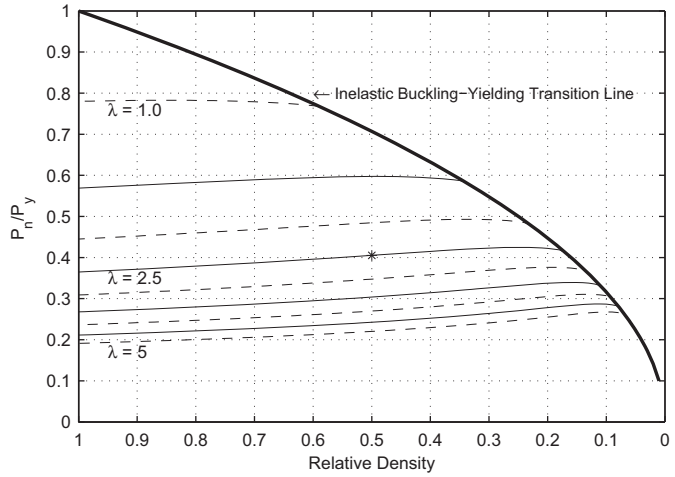

Fig. 4. Normalized plate collapse load in terms of solid plate relative density varying slenderness. The curves get higher as the plate slenderness is dropping.

The asterisk point in Figs. 2–4 corresponds to a specific plate with relative density equal to 0.5 and solid plate slenderness equal to 2.5.

By comparing these figures, it can be seen that for a given slenderness the collapse mechanism changes from buckling to crushing as the relative density is decreased, and that the buckling capacity increases with decreasing relative density. Thus, for slender plates, the use of steel foam presents two possible advantages: (1) a small increase in capacity if the failure mode is inelastic or elastic buckling and (2) a change from a buckling mode of failure to a more benign (and potentially more ductile) crushing mode of failure. One can see each of these possibilities by considering a plate with slenderness $\lambda = 2.25$ and observing that as the relative density is decreased the buckling capacity increases and then the failure mode changes to crushing. If the relative density is further decreased the failure mode remains crushing but the nominal strength decreases rapidly.

4. Steel foam lipped channel

In this part of the study, the response of a steel foam lipped channel under different loading conditions is investigated. The objective here is to find out whether replacing the solid steel walls of the lipped channel with steel foam walls can alter the response in potentially beneficial ways. The 362S162-68 and 362S200-54 cold-formed steel lipped channels (nomenclature per [6]) are chosen as the prototype cross-sections for the pure compression and bending simulations respectively. These cross sections are chosen to correspond to those used in existing experimental studies [12–14] for investigating the compressive and flexural behavior of lipped channels. Fig. 5 provides dimension of the prototypical sections. The steel elastic modulus and steel yield stress are chosen to be equal to $E_s = 2.03 \times 10^5$ MPa (29 500 ksi) and $f_{ys} = 345$ MPa (50 ksi) respectively. The postyielding behavior is assumed to be perfectly plastic.

4.1. Cross section properties of the steel foam lipped channel

In this section, the cross section properties of the 362S162-68 steel foam lipped channel are provided. Fig. 6 shows the variation of the cross section properties of steel foam lipped channel in terms of foam relative density. In this figure, the cross section properties are normalized by dividing them by cross section properties of the solid steel lipped channel. It can be seen that

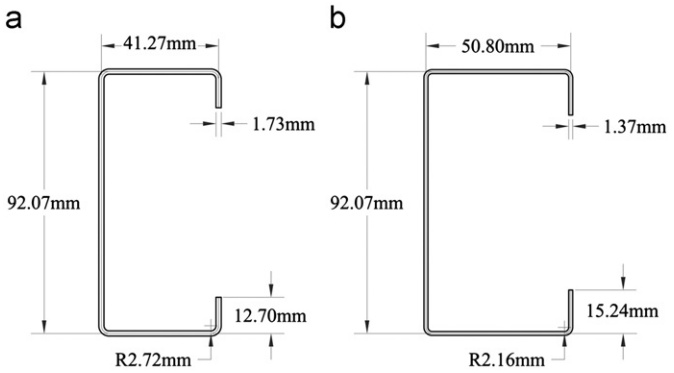

Fig. 5. Dimension of the (a) 362S162-68 and (b) 362S200-54.

the variations of A_f/A_s, I_f/I_s, and Cw_f/Cw_s, in terms of relative density are similar. Moreover, the variations of E_fA_f/E_sA_s, E_fI_f/E_sI_s and E_fCw_f/E_sCw_s in terms of relative density are similar as well. Axial stiffness (EA), bending stiffness (EI) and torsional buckling stiffness (ECw) of the steel foam lipped channel are reduced as relative density is decreased, while the torsional stiffness (GJ) increases when the relative density is decreased.

4.1.1. Local and global buckling resistance of the steel foam lipped channel

The elastic buckling strength of the lipped channel in a local mode is proportional to the plate bending rigidity $D_f = E_f t_f^3/(12(1-\nu^2))$. Using Eqs. (1) and (2), it can be found that

$$P_{cr,local} \propto \rho^{-1} \tag{15}$$

In the flexural global buckling mode of a steel foam lipped channel, on the other hand, the buckling strength is proportional to the weak axis bending stiffness $E_fI_{yy,f}$. The moment of inertia $I_{yy,f}$ can be approximated by

$$I_{yy,f} \approx \frac{2t_f b^3}{12} + 2dt_f\bar{x}^2 + ht_f(b-\bar{x})^2 + 2bt_f\left(\frac{b}{2}-\bar{x}\right)^2 \tag{16}$$

where $\bar{x}$ is the distance from the neutral axis of the section to the centerline of the lips. Since $I_{yy,f}$ is proportional to t_f which is in turn proportional to ρ^{-1}, and E_f is proportional to ρ^2, the flexural global buckling load obeys the proportionality

$$P_{cr,global} \propto \rho \tag{17}$$

Eqs. (15) and (17) show that a steel foam lipped channel is expected to exhibit greater local buckling capacity and less global buckling capacity than a solid steel channel with the same weight per unit length, as shown in Fig. 7.

4.2. Linear eigenvalue analysis

Linear eigenvalue analysis is performed on the lipped channels to determine the relationship between the elastic buckling load and the relative density. The analysis is performed using CUFSM [7] which employs the finite strip method and elements implemented following Kirchoff thin plate theory for bending and plane stress assumptions for membrane deformations. The finite strip method is a specialized version of the finite element method. In the finite strip method, element shape functions use polynomials in the transverse direction, but trigonometric functions in the longitudinal direction. This allows discretization only for the cross section and in the longitudinal direction a single element is sufficient. In Fig. 8 a single strip element with its degrees of freedom and applied edge tractions are shown. For the in-plane displacements, u and v, linear shape functions are used in the transverse direction, and in the longitudinal direction u uses a

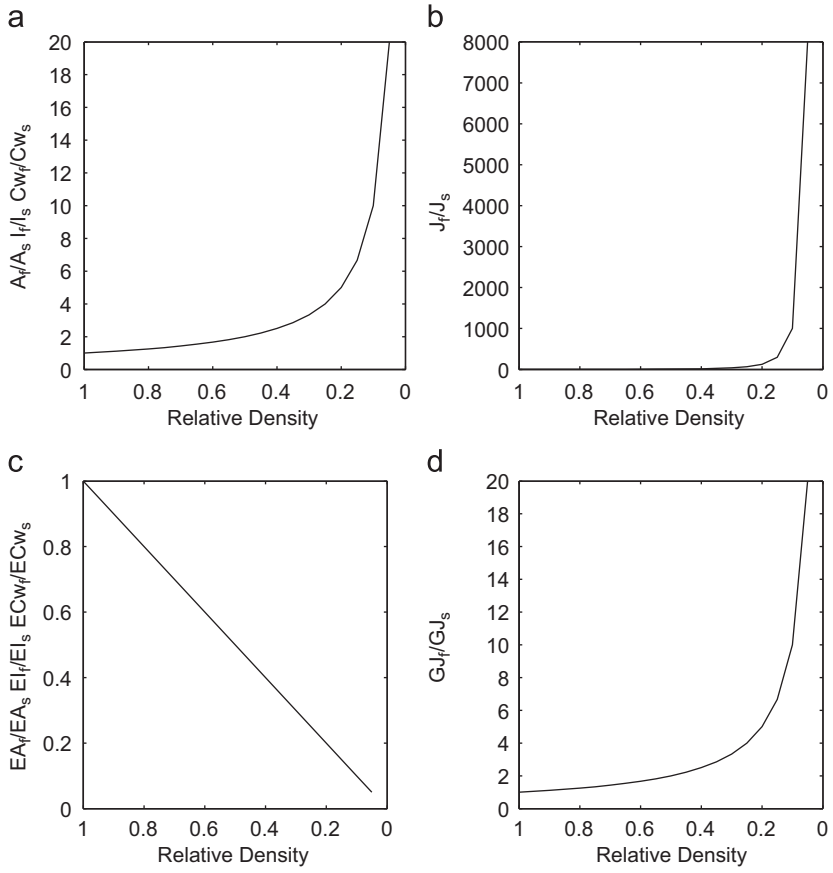

Fig. 6. Variation of cross section properties of steel foam lipped channel in terms of foam relative density.

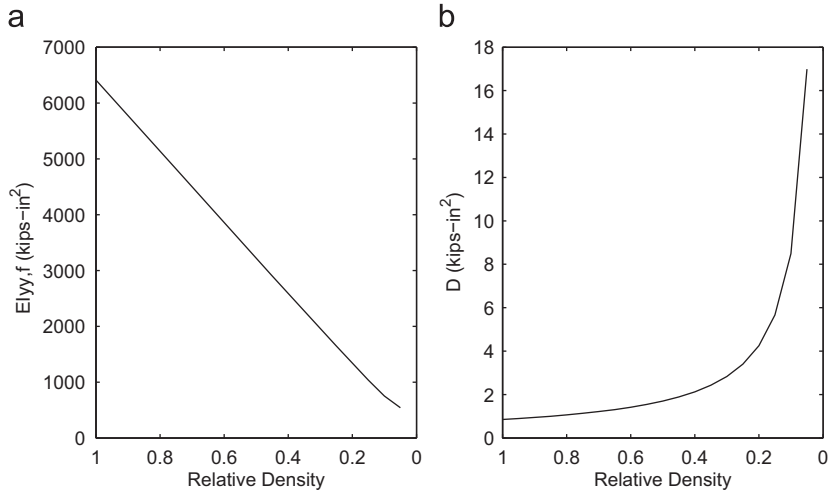

Fig. 7. (a) EI in global *Y* direction and (b) EI for the web plate in terms of relative density of the steel foam 362S162-68.

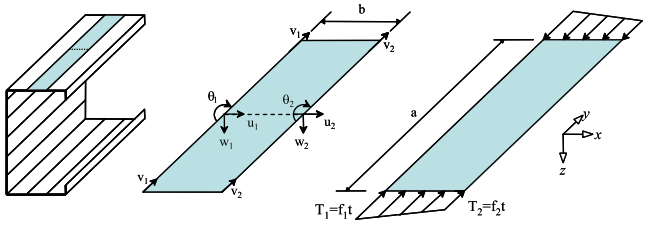

Fig. 8. Finite strip discretization, strip DOF, dimensions, and applied edge tractions [7].

sine function and v a cosine function. The out-of-plane displacement, w, is approximated by a cubic polynomial in the transverse direction and sine function in the longitudinal direction [7].

When the relative density of the 362S162-68 channel is 0.2, the width to thickness ratio of the web decreases from 50 to 11. Shear deformations are generally assumed to be negligible when this ratio is greater than 10. Therefore, CUFSM, which is implemented with thin plate bending assumptions, is appropriate for steel foam lipped channels with relative density as low as 0.2. For relative density of 0.05 (the lowest density examined herein), the

width to thickness ratio of the web is 2.6, implying that the shear deformations will be significant, and in this regime the finite strip implementation in CUFSM will overestimate the stiffness.

The primary output from a CUFSM buckling analysis of a member under a given loading (axial, bending, etc.) is the "signature curve" of buckling half-wavelength vs. buckling load factor. Each point in the signature curve corresponds to the buckling force (or moment) for a given half-wavelength and each half-wavelength is associated with a specific buckling mode (Figs. 9 and 10). The minima in the signature curve are of special interest, and correspond to the critical half-wavelength and buckling force for all possible buckling modes. There are usually two minima in the buckling curve of a lipped channel. The minimum with smaller half-wavelength corresponds to the local buckling mode and the minimum with larger half-wavelength corresponds to the distortional buckling mode. Local buckling is characterized by buckling of the lipped channel walls without transverse movement of the joints (fold locations). Distortional buckling is characterized by rotation of the flange at the flange/web junction. The trailing portion of the signature curve, at long half-wavelengths, is the global buckling mode, which may be recognized by the mode shape: the member bends or twists without change of the cross-sectional shape [7,8].

Fig. 9 shows the signature curve of the 362S162-68 lipped channel under pure compression and Fig. 10 depicts the buckling curve of the 362S200-54 under pure bending. Three buckling mode shapes can be seen in these figures and these curves should be kept in mind as the response of the steel foam lipped channels is described, since the relative density (amount of foaming) affects the different buckling modes in different ways.

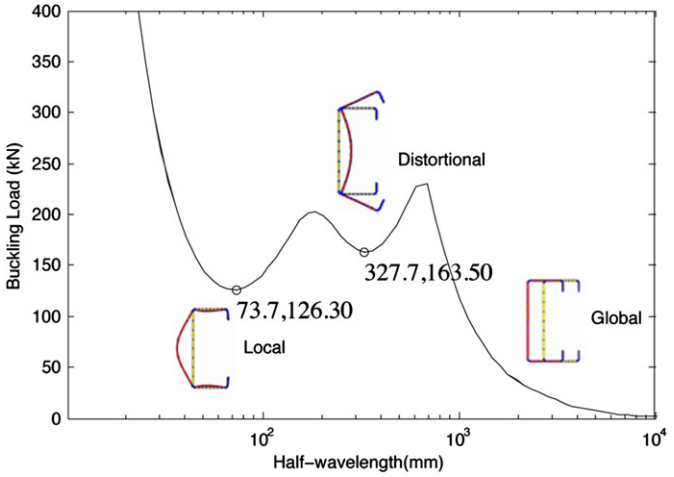

Fig. 9. Buckling curve of the 362S162-68 under pure compression.

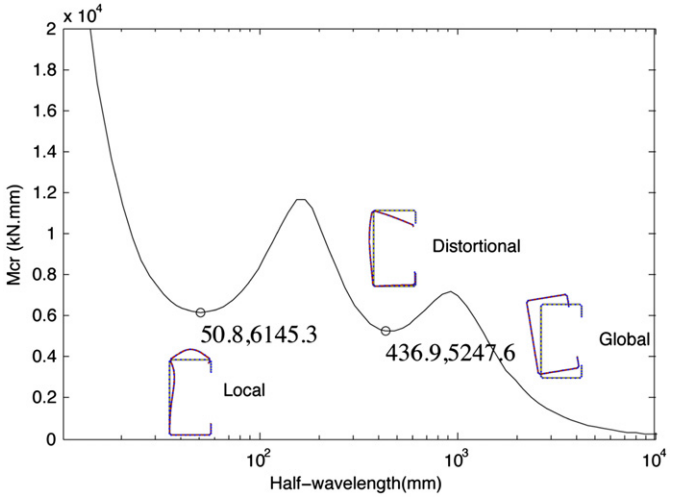

Fig. 10. Buckling curve of the 362S200-54 under pure bending.

4.2.1. Pure compression

Fig. 11 shows the series of buckling (signature) curves that are generated for the lipped channel over the full range of relative densities. These buckling curves are arranged to form a buckling surface that gives the buckling load as a function of half-wavelength and relative density (i.e. amount of foaming). There are two troughs in Fig. 11. The one centered at a smaller half-wavelength corresponds to local buckling and the second trough to distortional buckling. Half-wavelengths longer than that of the second trough buckle globally or in a mixed global-distortional mode. The sensitivity of buckling load to relative density for large half-wavelength is smaller than that for small half-wavelength.

In Fig. 11, the bold solid and dash line superimposed on the buckling surface represents the buckling load at an unbraced

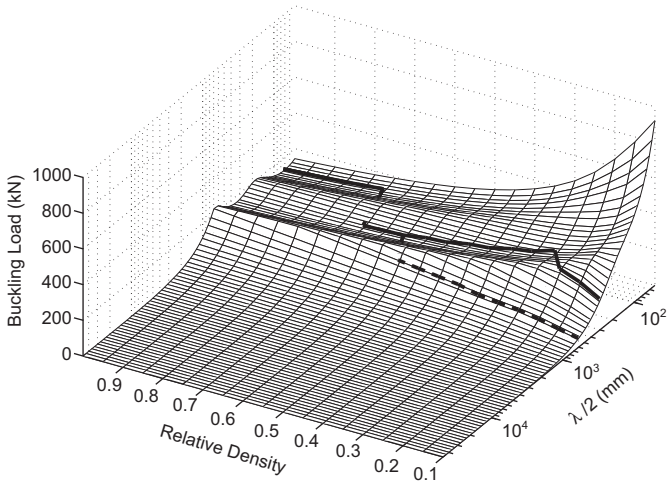

Fig. 11. Buckling surface showing relationship between buckling load, half wavelength (λ) and relative density under compression. The bold solid and dash line superimposed on the buckling surface represents the design buckling load at a unbraced length of 305 mm and 610 mm respectively.

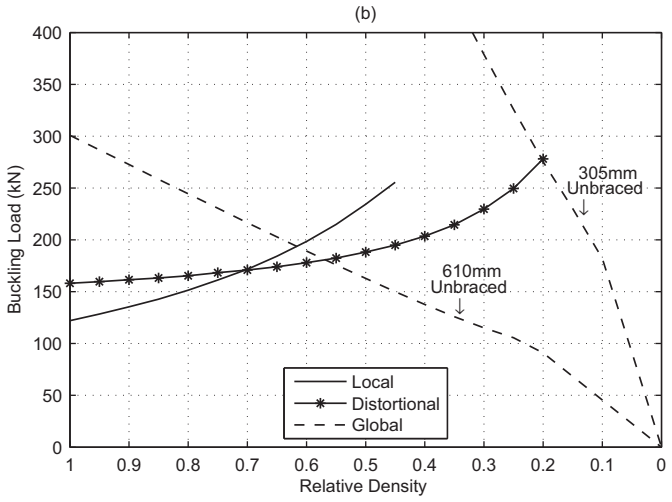

Fig. 12. Axial local–distortional–global buckling load of (a) the 305 mm (1 ft) and (b) the 610 mm (2 ft) unbraced length steel foam lipped channel in terms of steel foam relative density.

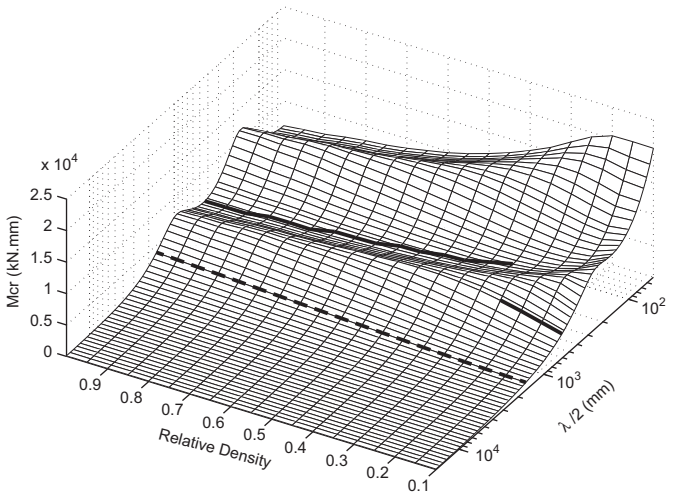

Fig. 13. Buckling surface showing relationship between critical moment, half wavelength (λ) and relative density under bending. The solid and dash line superimposed on the surface represents the critical moment for a 610 mm (2 ft) and 1626 mm (5-1/3 ft) design half-wavelength.

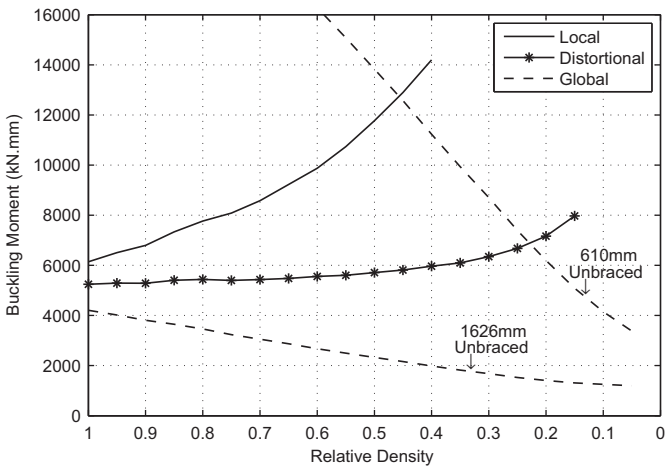

Fig. 14. Local–distortional–global critical moment of (a) the 610 mm (2 ft) and (b) the 1626 mm (5-1/3 ft) unbraced length steel foam lipped channel in terms of steel foam relative density.

length of 305 mm (1 ft) and 610 mm (2 ft) respectively over the range of relative densities. The buckling load at a given unbraced length is the minimum buckling load at that length or any smaller half-wavelengths.

Fig. 12 shows the local, distortional, and global buckling load of the 305 mm and 610 mm unbraced length steel foam lipped channel in terms of steel foam relative density under pure compression. A key observation is that as the relative density is decreased the dominant buckling mode changes from local to distortional then finally to global. The change in buckling mode is caused by the influence of foaming the steel, which increases the local buckling load, but decrease the global buckling load. While lower distortional and global buckling loads for the bare member are undesirable, these modes may be externally braced (and typically are in most cold-formed steel applications) while local buckling generally cannot be meaningfully restricted since it occurs over such a short length. In the balance, considering a complete application (e.g. sheathing bracing) the benefit in increasing local buckling may be worth the cost of decreases in global buckling.

4.2.2. Pure bending

Fig. 13 shows the relationship between steel foam relative density, half-wavelength and critical moment of the steel foam lipped channel in bending. Similar to the troughs in the buckling surface of the lipped channel under compression, the troughs in the buckling surface of the lipped channel under pure bending correspond to local and distortional buckling. The sensitivity of buckling load to relative density for large half-wavelength is smaller than that for small half-wavelength. The bold solid and dashed line superimposed on the buckling surface represent the buckling load at an unbraced length of 610 mm (2 ft) and 1626 mm (5-1/3 ft) respectively over the range of relative densities.

Fig. 14 shows the local, distortional, and global critical moment calculated using the FSM approach for the 610 mm (2 ft) and 1626 mm (5-1/3 ft) unbraced length steel foam lipped channel. It can be seen that replacing the solid steel walls of the original channel with steel foam increases the distortional and local buckling resistance of the channel under pure bending. On the other hand the global buckling load decreases. For the 610 mm (2 ft) unbraced length member, when the relative density is reduced, the buckling mode changes from distortional to global. There is almost no change in buckling resistance until relative density reaches 0.25 and then buckling resistance decreases. This change of mode is again potentially advantageous since it is easier to brace against global buckling than distortional buckling. The 1626 mm (5-1/3 ft) unbraced length member buckles globally for all relative densities, so replacing steel walls with steel foam always reduces the buckling resistance of the 1626 mm (64 in) unbraced length lipped channel under pure bending if it is unbraced. Only if the member is braced against lateral–torsional buckling can the advantageous increases in local and distortional buckling resistance due to foaming be realized.

4.3. DSM-based nominal strength

In this section the nominal strength of the lipped channel is determined using the Direct Strength Method (DSM) [4]. Three axial nominal strengths P_{ne}, P_{nl} and P_{nd} correspond to global, local (with global interaction), and distortional buckling respectively and three nominal flexural strengths M_{ne}, M_{nl} and M_{nd} correspond to lateral–torsional, local, and distortional buckling respectively. The DSM employs the buckling loads and empirical strength curves to provide the nominal member strength in each limit state [4].

4.3.1. Nominal axial strength

The yield strength of the steel is assumed to be 345 MPa (50 ksi), Eq. (7) is used to determine the effective squash load of the foamed steel, P_{nf}. Fig. 15 shows the nominal axial strengths of the 305 mm (1 ft) and 610 mm (2 ft) unbraced length steel foam lipped channel in terms of relative density. Reducing the relative density (foaming the steel) decreases the minimum nominal axial strength. Even at 305 mm (1 ft) length the loss in effective yield strength for the foamed steel (i.e. the decrease in P_{nf}) is more detrimental than the benefits incurred in P_{crl} and P_{crd}. The change in failure mode from inelastic buckling to yielding/crushing may be beneficial from a ductility standpoint, but the predicted capacity loss is disappointing.

4.3.2. Nominal flexural strength

Fig. 16 shows the nominal flexural strength for local, distortional and global buckling obtained from DSM for the 610 mm

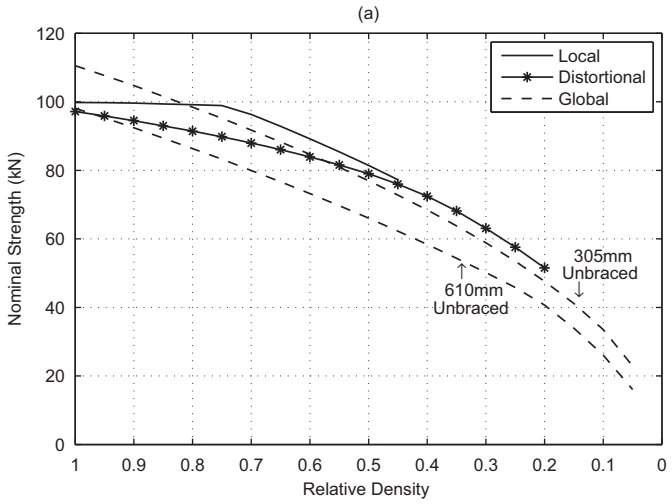

Fig. 15. The nominal axial strength for local, distortional and global buckling for (a) 305 mm (1 ft) and (b) 610 mm (2 ft) unbraced length steel foam lipped channel in terms of steel foam relative density (using DSM equations).

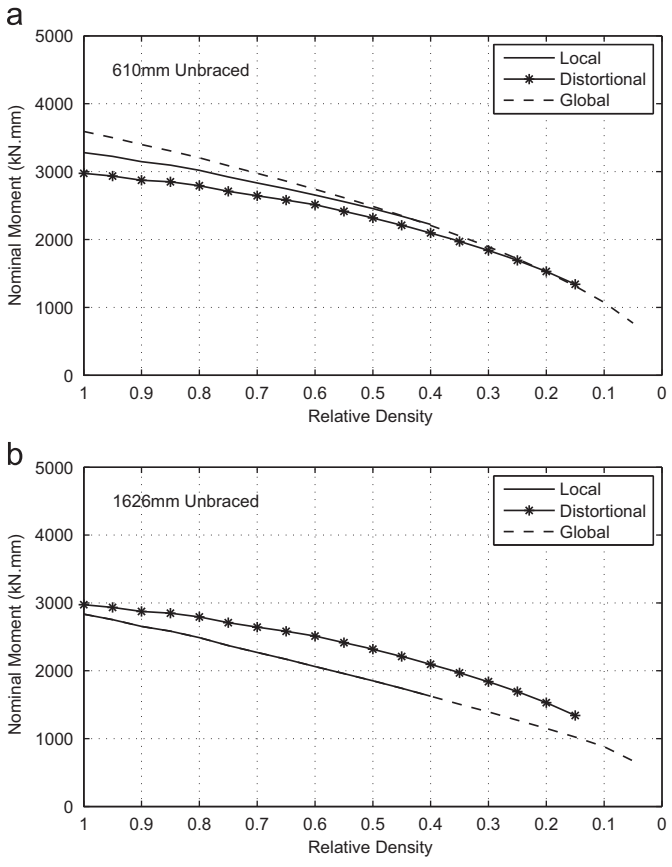

Fig. 16. The nominal flexural strength for local, distortional and global buckling for (a) 610 mm (2 ft) and (b) 1626 mm (64 in) unbraced length steel foam lipped channel (using DSM equations).

(2 ft) and 1626 mm (5-1/3 ft) unbraced length steel foam lipped channel. As in the case of pure axial loading, the benefit to the elastic critical loads in the local and distortional modes is lost when nominal strengths are calculated using the DSM.

The normalized inelastic strain ratio (C_y) which is the ratio of engineering failure strain to yielding strain (Eq. (18)) has been established as a measure of the energy absorption capacity of structural members, specifically cold-formed steel lipped channels [11].

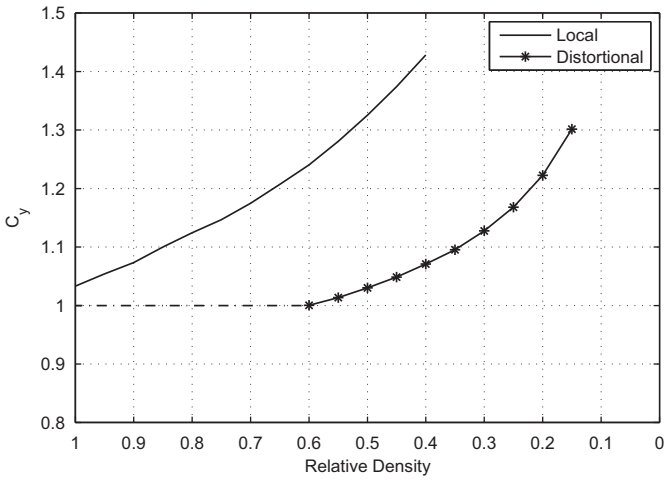

Fig. 17. C_{yl} and C_{yd} in terms of relative density.

$$C_y = \frac{\epsilon_{failure}}{\epsilon_{yield}} \tag{18}$$

It can be seen in Fig. 17 that as relative density is decreased, C_y increases significantly. We can therefore conclude that although steel foam channels may not deliver substantial increases in member strength, they may have substantially different load-deformation characteristics, leading to far greater amounts of energy absorption prior to collapse. This could be a very useful feature of such elements for mitigation of catastrophic structural collapse.

5. Conclusion

The manufacture of foamed steel structural members is now a real possibility, and this paper explores the potential for foamed steel to be productively used as a thin-walled structural member. Using theoretically derived relationships for the basic material properties of foamed steel, both plates and thin-walled lipped channels are explored.

For steel foam plates loaded with in-plane compression it is shown that the elastic local buckling load benefits from the foaming; however, the crushing/yielding load of the same plate decreases. The plate relationships may be written in closed-form and provide a direct means of understanding how relative density, i.e., the degree to which the plate is foamed, impacts the performance. Winter's equation has been used to evaluate plate behavior because it is widely used in design and has been shown to provide accurate, conservative, predictions of experimentally measured plate strengths.

For thin-walled members, closed-formed expressions are not convenient as the local, distortional, and global buckling loads (or moments) that dominate the performance of these members are most conveniently provided numerically. Using prototypical cold-formed steel members, the influence of foaming on the buckling loads, strength, and ductility of both a column and a beam are explored. Foaming the steel increases the local buckling load, may increase or decrease the distortional buckling load, and decreases the global buckling load. Local buckling is essentially plate buckling, and follows the closed-formed relations established. Global buckling may be understood to rely on integral properties of the cross-section, and these are not benefited by the foaming. Distortional buckling, which is a mode where some of the buckling mode deformations are plate-like and some member-like; essentially must

be taken on a case-by-case basis. The elastic buckling analysis of the thin-walled lipped channels has been conducted using the finite strip method, which is an allowed method of calculation in the AISI design specification.

When strength is considered (using the AISI Direct Strength Method) the benefits of the foaming are decreased significantly, the loss in effective yield/crushing load (or moment) results in losing many of the observed benefits. An important exception exists: members which have external bracing (e.g., sheathing or drywall) that may restrict global, or distortional buckling – a situation that is common in actual applications – may still benefit significantly from the local buckling improvements from foaming. In general, foaming the steel makes yielding/crushing modes far more prevalent. This, in turn, results in greatly enhanced ductility—as illustrated herein for the large increases in the ratio of the predicted failure strain to the strain at first yield for steel foam sections. Thin-walled steel foam members provide the possibility of enhanced local stiffness, increased local buckling loads, and increased ductility. However, this must be carefully balanced against potential loss in maximum load carrying capacity, particularly for bare steel members. Further study of these members is warranted and underway.

Acknowledgments

Moradi and Arwade wish to thank Mr. Robert Brack for his generous support of the Department of Civil and Environmental Engineering at the University of Massachusetts. Arwade and Schafer would like to thank the United States National Science Foundation for financial support through Grants CMMI:1000334 and 1000167.

References

[1] Rabiei A, Vendra LJ. A comparison of composite metal foam's properties and other comparable metal foams. Materials Letters 2009;63:533–6.
[2] Park C, Nutt SR. Anisotropy and strain localization in steel foam. Materials Science and Engineering A 2001;299:68–74.
[3] Kremer K, Liszkiewicz A, Adkins J. Development of steel foam materials and structures. US DOE and AISI Final Report DE-FC36-97ID13554 performed by Fraunhofer USA Delaware Center for Manufacturing and Advanced Materials, Newark, DE; 2004.
[4] North American Specification for the design of cold-formed steel structural members, AISI-S100 Appendix 1 2007 ed. American Iron and Steel Institute (AISI).
[5] Ashby M, Evans A, Fleck N, Gibson L, Hutchinson J, Wadley H. Metal foams: a design guide; 2000.
[6] Steel Stud Manufacturers Association. ICBO ER-4943P.
[7] Li Z, Schafer BW. Buckling analysis of cold-formed steel members with general boundary conditions using CUFSM: conventional and constrained finite strip methods. In: Proceedings of the 20th international specialty conference on cold-formed steel structures, St. Louis, MO, November 2010.
[8] Schafer BW, Pekoz T. Computational modeling of cold-formed steel: characterizing geometric imperfections and residual stresses. Journal of Constructional Steel Research 1998;47:193–210.
[10] Ashby M, Gibson L. Cellular solids: structure and properties, 2nd ed., 1999.
[11] Shifferaw Y, Schafer BW. Inelastic bending capacity in cold-formed steel members. In: Proceeding of the annual technical session and meeting. New Orleans, LA: Structural Stability Research Council; April 2007. p. 279–99.
[12] Yu C, Schafer BW. Local buckling tests on cold-formed steel beams. ASCE, Journal of Structural Engineering 2003;129(12):1596–606, http://dx.doi.org/10.1061/(ASCE)0733-9445(2003)129:12(1596).
[13] Yu C, Schafer BW. Distortional buckling tests on cold-formed steel beams. ASCE, Journal of Structural Engineering 2006;132(4):515–28, http://dx.doi.org/10.1061/(ASCE)0733-9445(2006)132:4(515).
[14] Vieira jr. LCM, Shifferaw Y, Schafer BW. Experiments on sheathed cold-formed steel studs in compression. Journal of Constructional Steel Research 2011;67:1554–66.
[15] Smith BH, Szyniszewski S, Hajjar JF, Schafer BW, Arwade SR. Review: steel foam for structures: a review of applications, manufacturing and material properties. Journal of Constructional Steel Research, 2012;71:1–10.
[16] Kalyanarama V, Pekšz T, Winter G. Unstiffened compression element. ASCE, Journal of the Structural Division 1977;103(ST9):1833–48.
[17] Schafer BW. Designing cold-formed steel using the direct strength method. In: Eighteenth international specialty conference on cold-formed steel structures, Orlando, FL, October 2006.